Integrating Unbiased Path Sampling with Biased Enhanced Sampling for Rare-event Kinetics

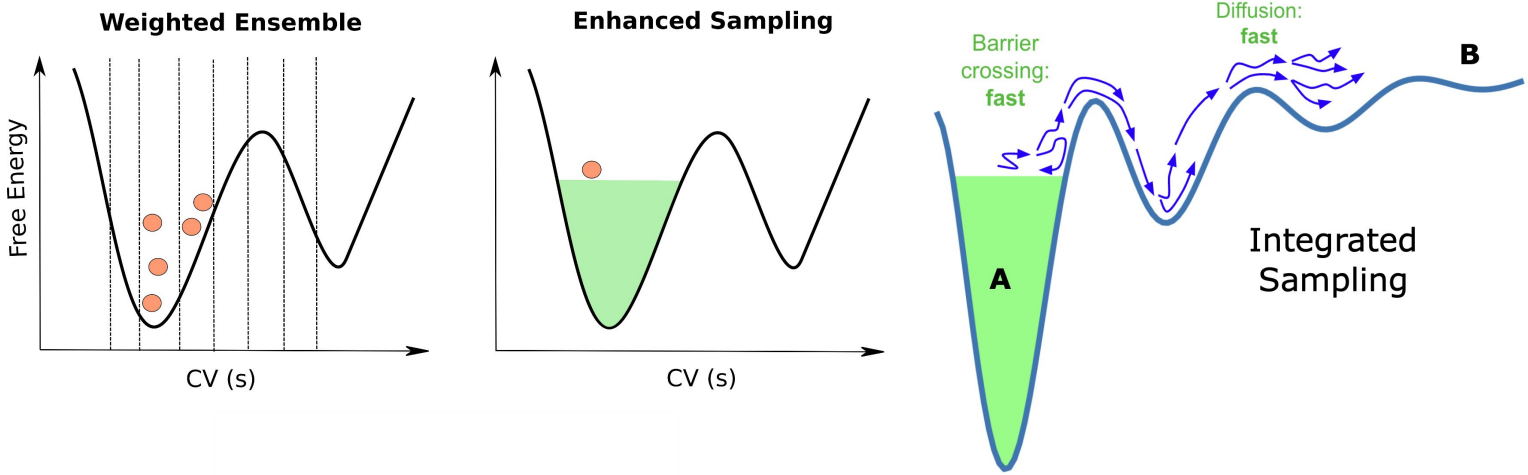

Dhiman Ray

Assistant Professor

Department of Chemistry and Biochemistry

University of Oregon

Memories

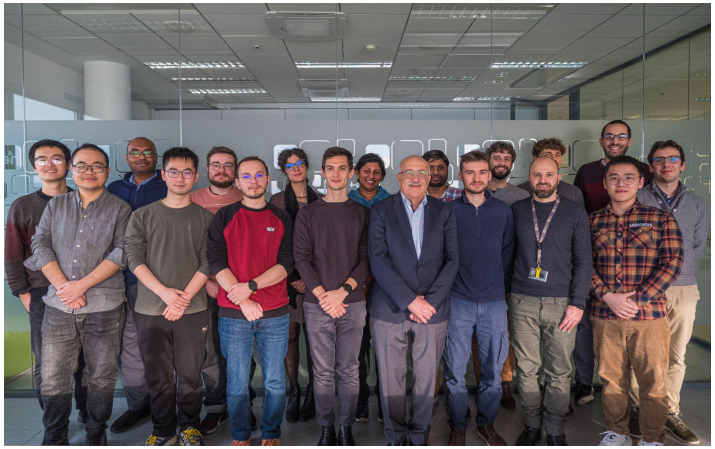

Parrinello Group in 2024

The Ray Computational Biophysics Group

Since September 2024

Department of Chemistry and Biochemistry

Material Science Institute

Department of Physics and Astronomy

https://blogs.uoregon.edu/dhimanraygroup/

The Ray Computational Biophysics Group

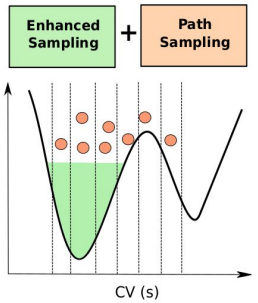

Integrating Enhanced Sampling and Path Sampling Algorithms

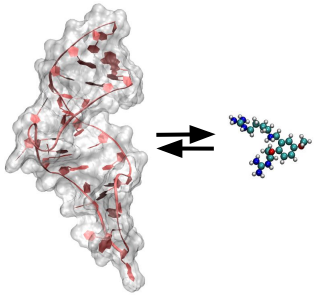

RNA-targeted drugs to combat antibiotic resistance

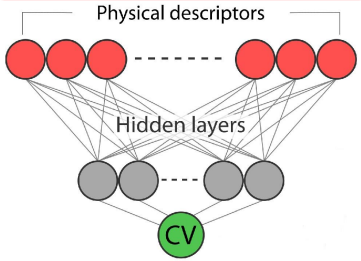

Machine Learning for Collective Variable Discovery

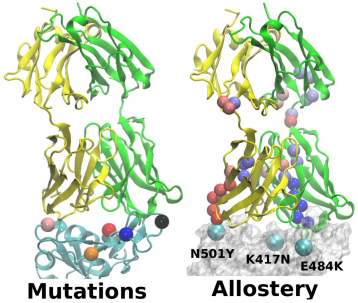

Mechanistic Study of Antigen-Antibody Recognition

Department of Chemistry and Biochemistry

Material Science Institute

Department of Physics and Astronomy

https://blogs.uoregon.edu/dhimanraygroup/

Introduction to rare event kinetics

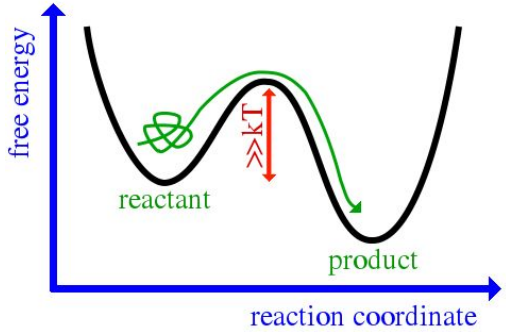

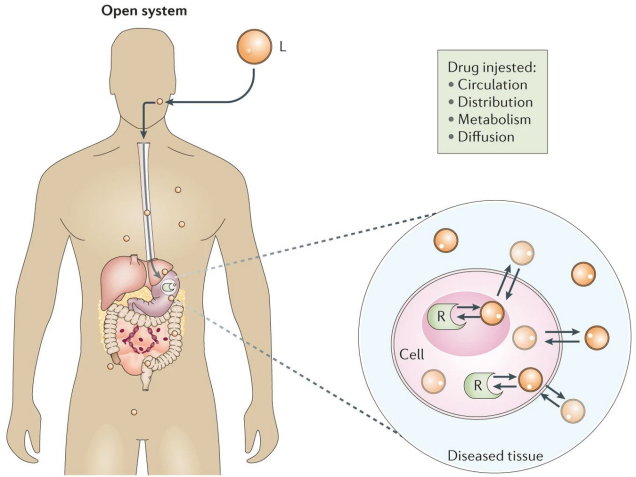

Free Energy

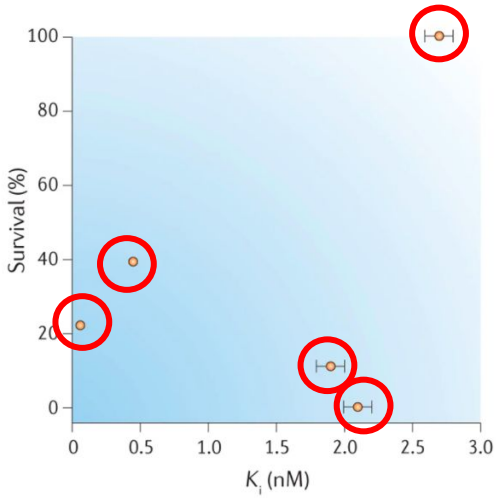

Kinetics

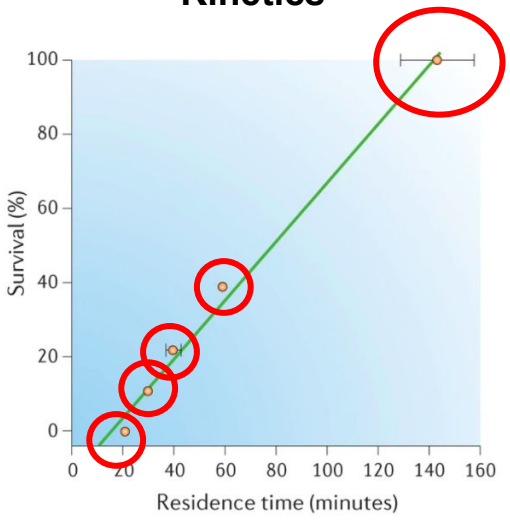

Action of a therapeutic drug is more correlated with residence time (kinetics) than free energy

Applying biasing force distorts the natural dynamics and kinetic properties

Guo et al. Br. J. Pharmacol. (2012), Copland et al. Nat. Rev. Drug. Disc. (2006), Laio & Parrinello PNAS, (2002),Tiwary and Parrinello PRL (2014)

Biased Conformational Flooding approach

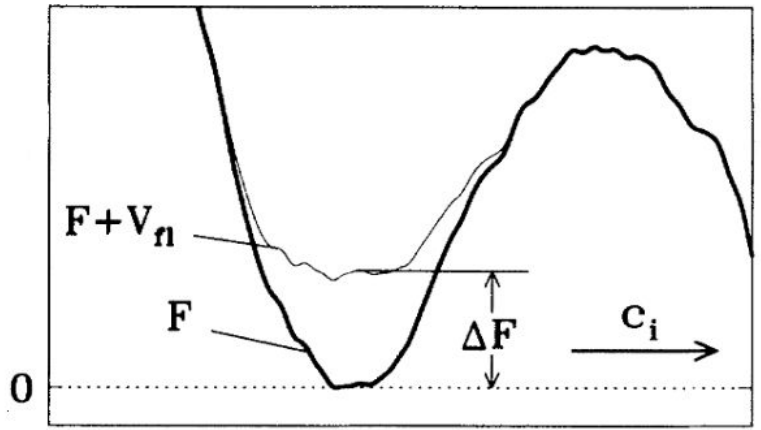

FIG. 2. "Conformational flooding" lowers free energy barriers of CT's and thus should accelerate the transitions. The

Grubmuller, PRE, September 1995

How to calculate rate constant from flooding?

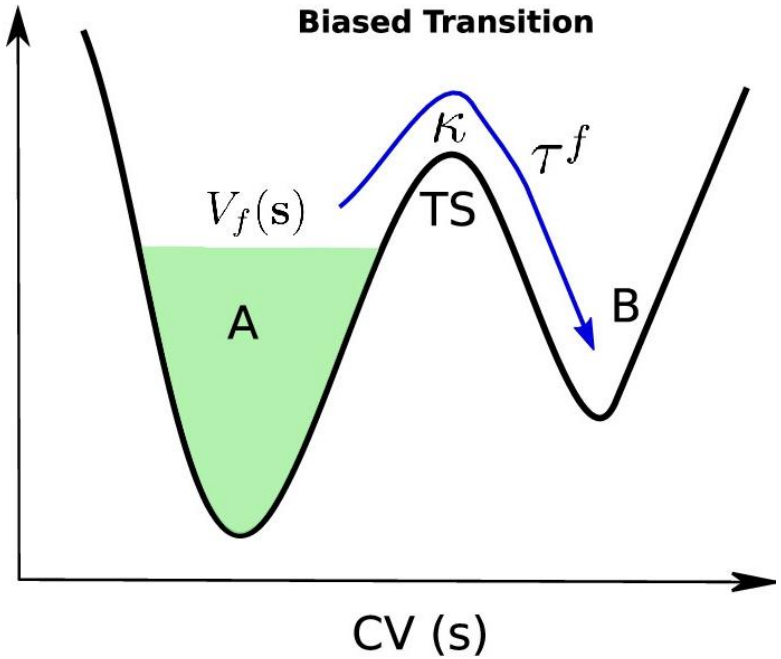

$$\frac{1}{\tau^f} = \omega\kappa\frac{Z_{TS}}{Z_0^f}$$

Assumptions

- Transition state unaffected by flooding bias
- Transmission coefficient κ is not affected by flooding

$$\frac{\tau}{\tau^f} = \langle \exp(\beta V_f(\mathbf{R})) \rangle_{U+V_f}$$

Average computed over initial state basin

Tiwary and Parrinello, PRL (2013), McCarty et al. PRL (2015), Ray and Parrinello, JCTC (2023)

CV based approach: Infrequent metadynamics

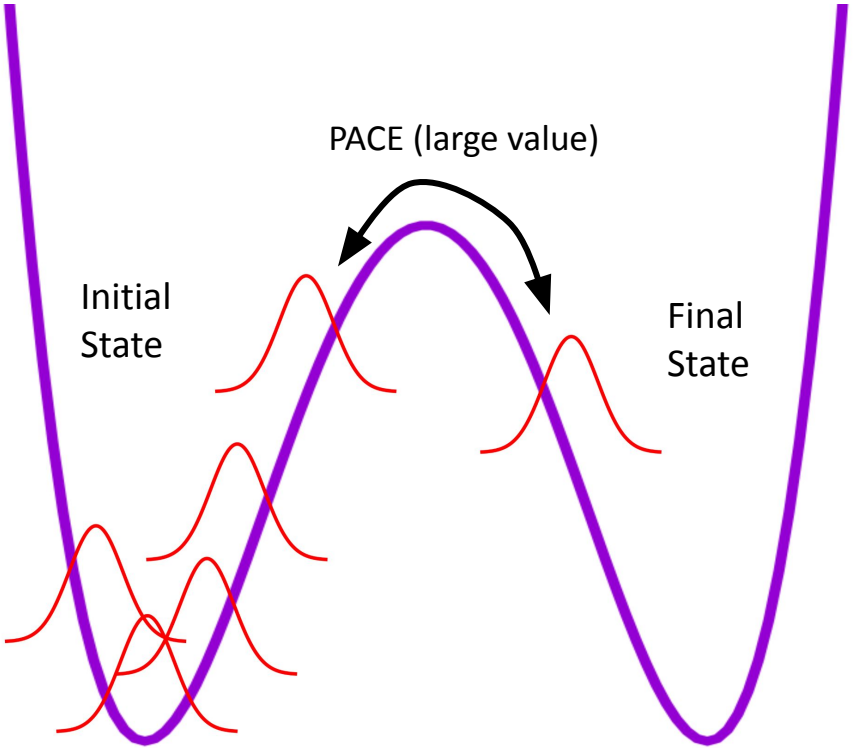

- Metadynamics with higher PACE (low frequency of Gaussian bias deposition)
- “Hope” that no bias will be deposited on TS which is short-lived

Tiwary and Parrinello PRL 2013, Salvalaglio et al. JCTC 2014

And a large body of literature in biology, material and chemical systems

Kinetics from Metadynamics: Principles, Applications, and Outlook

Dhiman Ray* and Michele Parrinello*

Cite This: J. Chem. Theory Comput. 2023, 19, 5649−5670

Read Online

Ligand binding

Table 1. Summary of Ligand Unbinding Kinetics (k_{off}) Computed Using Infrequent Metadynamics and Related Approaches

Receptor−Ligand (PDB ID)	Force Field	Method and CV Description	Computed k_{off} or Residence Time	Experimental k_{off} or Residence Time	Year and Reference
Trypsin-Benzamidine (2OXS)	Protein: AMBER99SB-ILDN, Ligand: GAFF-RESP	a torsion CV and the z component of a contact map path CV	8.1 ± 2.3 s^{-1}	680 ± 300 s^{-1}	2015 (ref 160)
Hydrophobic Cavity Model Ligand	Leonard-Jones	center of mass distance between ligand and cavity	200 ± 51 s	-	2015 (ref 161)
Hydrophobic Cavity Model Ligand	Leonard-Jones, explicit TIP4P water, OPLS	SGOOP CV trained on 3 OP: distance of ligand along surface-normal (z), the distance between the projection of the ligand on the surface and the binding cavity, and no. of water molecules in the cavity.	∼2000 s	∼2000 s	2016 (ref 76)
L99 T4 Lysozyme-Benzene	Protein and Ligand: CHARMM36-23*	Path CV on the contacts between ligand and binding pocket	7 ± 2 s^{-1}	800 ± 200 s^{-1}	2017 (ref 98)
RNA Aptamer-theophyline (1SH7)	AMBER99SB	COM distance between the binding pocket and ligand and solvent coordination of the ligand	Three different situations based on experiments: (i) 54 ± 45 s, (ii) 45 ± 39 s, and (iii) 750 ± 730 ms	(i) (ii) 14 s, (iii) 50 ms	2017 (ref 111)
c-Src kinase-Dasatinib (3G5D)	OPLS AA force field	distance of the drug from the binding pocket and the solvation state of the binding pocket	21 ± 10 s	18 s	2017 (ref 47)
p38 MAP kinase-Inhibitor (fragment of the drug BIRB 796) (3HV2)	Protein: AMBER ff99SB-ILDN, Ligand: GAFF with RESP charges (HO/6-31G(d))	Three CV combinations: (i) distance between the binding pocket and ligand, (ii) pocket-ligand distance and ligand solvation, (iii) Path CV on contacts between ligand and protein residues	(i) (ii) 14 ± 4 (iii) 10^{-4} s^{-1} (p = 0.02) (ii) 0.020 ± 0.011 s^{-1} (p = 0.40) (iii) 0.04 ± 0.03 s^{-1} (p = 0.77)	0.34 s^{-1}	2017 (ref 73)
HIV Protease-Lopinavir (1MUI)	Protein: AMBER ff99SB-ILDN, Ligand: GAFF with HF/6-31G(d) RESP charges	2D CV used for biasing: CV1: distance between binding pocket and drug, CV2: RMSD change of the active pocket	7.66 × 10^{-4} s^{-1}	6.50 × 10^{-4}	2017 (ref 102)
HIV Protease-Atazanavir (1ZXZ-C)	same as above	same as above	5.57 × 10^{-4} s^{-1}	6.90 × 10^{-4} s^{-1}	2017 (ref 102)
HIV Protease-Indinavir (3WSJ)	same as above	same as above	1.11 × 10^{-3} s^{-1}	1.60 × 10^{-3} s^{-1}	2017 (ref 102)
Renin-Aliskiren (2 VSZ)	same as above	same as above	8.18 × 10^{-4} s^{-1}	1.10 × 10^{-3} s^{-1}	2017 (ref 102)
EGFR-Lapatinib (3BRT)	same as above	same as above	4.77 × 10^{-3} s^{-1}	3.90 × 10^{-3} s^{-1}	2017 (ref 102)
Neurotransmitter-Oxaltomivir (4HEZ)	same as above	same as above	2.00 × 10^{-3} s^{-1}	2.30 × 10^{-3} s^{-1}	2017 (ref 102)
Streptavidin (WT, N23A)-Biotin (3RY2)	Protein: Amber ff99SB*-ILDN, Ligand: GAFF with AM1-BCC charges	1D SGOOP CV built using 5 OPs involving distances between protein and ligand atoms and hydration state of pocket residues	WT: 2.1 ± 1.5 s^{-1}, N23A: 218 ± 82 s^{-1}	WT: (4.4 ± 0.3) × 10^{-1} s^{-1}, N23A: (1850 ± 220) × 10^{-3} s^{-1}	2017 (ref 62)
L99 T4 Lysozyme-Benzene (3DWV)	Protein and ligand: CHARMM36	CV: COM distance between binding pocket and ligand	270 ± 100 s^{-1}	950 ± 20 s^{-1}	2018 (ref 99)
L99 T4 Lysozyme-Benzene	Protein: CHARMM22*, Ligand: CGENFF	1D CV obtained from SGOOP dimensionality reduction from 11 distances between protein residues and the ligand	1.5 ± 0.7 s^{-1}	950 ± 20 s^{-1}	2018 (ref 83)
L99 T4 Lysozyme-Benzene	Protein: CHARMM22*, Ligand: CGENFF	Frequency adaptive metadynamics with CV same as ref 98	176 ± 68 ms	∼1.05 ms	2018 (ref 16)
L99 T4 Lysozyme-Indole	same as above	same as above	168 ± 95 ms	3.0 ms (325 ± 75 s^{-1})	2018 (ref 16)
Subtilisase Ashalgarase (Ba4, Ligand: 2,5-dichloropropan-1-ol (DCP) (4E6K)	Protein: AMBER ff12SB, Ligand: GAFF	The z component of Path CV and COM distance between pocket and ligand.	1.01 ± 0.58 × 10^6 s^{-1}	∼10^6 s^{-1}	2019 (ref 113)
Subtilisase Ashalgarase (Ba4A1 mutant, Ligand: 2,3-dichloropropan-1-ol (DCP) (5B4A)	same as above	same as above	2.8 ± 1.2 × 10^5 s^{-1}	-	2019 (ref 113)
Trypsin-Benzamidine (2OXS)	AMBER: 14SB, GAFF, TIP3P	2 slowest modes of VAC-MetaD optimized CV form the following basis: (1) number of contacts between protein−ligand, (2) water molecules in the pocket, (3) ligand torsion angle, and (4) solvation of the ligand	4178 ± 334 s^{-1}	680 ± 300 s^{-1}	2019 (ref 77)
FKBP-BUT (1D7H)	Protein: AMBER99SB-ILDN, Ligand: GAFF	1D SGOOP CV from interatomic distances within and between the ligand and the binding pocket	27.3 ± 0.1 ns	21.3 ± 0.2 ns (unbiased MD)	2019 (ref 84)

Other biological processes

Table 2. Summary of Studies Involving Metadynamics Based Methods to Study the Kinetics of Biological Processes Other than Ligand Receptor Binding

Other Processes (Protein Folding etc.)	Method	Result	Year and Reference
Helix folding	Collective variable driven hyperdynamics (CVHD).	Dynamic reweighting and static bias both give folding kinetics in agreement with unbiased simulation	2015 (ref 60)
Unfolding of Chignolin and villin headpiece (HP35) protein	C-alpha RMSD from crystal structure as CV to drive unfolding. CHARMM22* for validation studies, and AMBER99SB-ILDN force field for studies in presence of ionic liquid (IL).	Chignolin 2.1(0.5) and HP35 0.83(0.2) μs without IL. Unbiased kinetic data from Shaw and co-workers:[111] 2.2(4) and 0.9(2) respectively (up to 400 fold speedup). Unfolding time decreases when IL is present.	2016 (ref 116)
Helix−coil transition in WHS peptide with sequence Ac-WAAAH$^+$-NH2)	3 different protein force fields (AMBER03, AMBER99, CHARMM22) and 2 different water models (TIP3P and TIP4P/2005) were tested. The ϕ and ψ backbone dihedral angles of the three central amino acids of the WHS peptide were used as CV.	Folding time: 50−400 ns, unfolding time: 1−7 ns. Slower folding and unfolding using TIP4P water model and faster (un)folding unfolding with CHARMM22 force field.	2016 (ref 117)
Diffusion of Meropenem antibiotic through $E. coli$ membrane channel OmpF	Infrequent Metadynamics with 2D CV space. CV1: distance between the protein and the small molecule projected along the normal of the membrane surface, CV2: orientation of substrate. The protein was modeled with the AMBER 99SB-ILDN force field, and the antibiotic was modeled with GAFF.	Computed escape time ∼550 ns is in good agreement with single channel experiment (1500 ± 400 ns).	2016 (ref 118)
Conformational transition in L99A mutant and L99A, G113A, R119P triple mutant of T4 lysozyme	Protein force field: CHARMM22*, CV: Path CV interpolating structures sampled between G and E states using MOIL.[119] Half-harmonic restraint is applied along the z component of the path CV.	Time scales of transition in L99A: G to E state: 175 ± 6 ms (experimental value: 20 ms), E to G state: 1.4 ± 0.6 ms (experimental value: 0.7 ms). Time scales of transition in triple mutant: G to E state: 2.0 ± 1.7 ms (experimental value: 0.2 ms), E to G state: 14.3 ± 8.3 ms (experimental value: 4 ms).	2016 (ref 75)
Kramers turnover: Kinetics of barrier crossing in energy diffusion and spatial diffusion regime	Langevin dynamics on two-dimensional toy model system proposed by De Leon and Berne.[120]	Infrequent metadynamics provides results in agreement with unbiased results across the energy diffusion to spacial diffusion regime (low to high friction) as long the bias deposition frequency is larger than the relaxation times of the orthogonal CVs.	2016 (ref 121)
Unfolding of chignolin mini-protein	Variational flooding in combination with infrequent metadynamics with 2D CV space comprised of NMR S3 parameter and native H-bonds contact map. CHARMM22* force field was used for the protein.	Unfolding time scales 1.9 μs at 340 K, 8.1 μs at 320 K, and 19.0 μs at 300 K (time scale from unbiased reference at 340 K: 2.2 ± 0.4 μs[122]).	2017 (ref 65)
Activation (conformational transition) of G protein-coupled receptor	CV: Protein is modeled with the CHARMM36m force field. Standard (no infrequent) metadynamics bias have been applied along a Path CV generated from structures sampled through adaptive bias MD simulation. Maximum caliber approach is used to reconstruct a Markovian kinetic model from the free energy surface.	Time scales of around 100s of ns were calculated between active, inactive, and intermediate states of GPCR.	2018 (ref 74)
Coupled folding and binding of intrinsically disordered protein p53 with MDM2	Amber99SB-ILDN CV1: COM distance, CV2: Coordination number of Phe19, CV3: Summation of the coordination numbers of Trp23 and Leu26.	Computed results: k_{off} 0.7 ± 0.4 $s^{-1}$$k_{on}$ (4.3 ± 2.2) × 10^6 M^{-1} s^{-1}. Experimental results: k_{off} 2.06 ± 0.09 s^{-1}, k_{on} (9.2 ± 0.04) × 10^5 M^{-1} s^{-1}].	2020 (ref 122)
Folding and unfolding of chignolin	OPES Flooding simulation with HLDA CV from ref 123, and Deep-LDA CV and Deep-TICA CV trained on 210 dimensional descriptor space from ref 88.	Time scales from different CVs:	2022 (ref 43) plumID:22.031
		HLDA: Folding: 1.74 μs, Unfolding: 6.33, μs. Deep-LDA: Folding: 1.89 μs, Unfolding: 2.93, μs.	
	CHARMM22* force field was used for the protein.	Deep-TICA: Folding: 1.28 μs, Unfolding: 3.21, μs. Unbiased reference:[123] Folding: 0.6 ± 0.1 μs, Unfolding: 2.2 ± 0.4 μs.	
Unfolding of chignolin	OPES Flooding simulation with Deep-TDA CV trained on 45 pairwise contacts between C_α atoms.	OPES: 3.08 μs (95% confidence interval: 1.94−4.70 μs),	2023 (ref 52) plumID:23.009
	CHARMM22* force field was used for the protein.	Unbiased reference:[123] Folding: 0.6 ± 0.1 μs, Unfolding: 2.2 ± 0.4 μs	

Chemistry and Materials

Table 3. Summary of the Application of Metadynamics-Based Methods in Studying the Kinetics of Chemical Reactions and Material Processes

Process	Method	Results	Year and Reference
Microscopic dissolution from aspirin water interface	Collective Variable Driven Hyperdynamics (CVHD). CV: center-of-mass (COM) vector of the link site molecule that triggers the escape of the molecule from its original location.	Dissolution time scale ∼1.3 μs	2014 (ref 135)
S_N2 reaction: $CH_3Cl + Cl^- \leftrightarrow CH_3Cl + Cl^-$	Ab initio MD at PM6 level of theory and Car−Parrinello MD at DFT level with BLYP functional.	Kinetics results are consistent with Arrhenius behavior	2015 (ref 136)
CH_4 dissociation on Ni(111) surface	CVHD with ReaxFF force field, CV: Stretching degree of freedom of the bonds.	process reaction time $CH_4(g) \rightarrow CH_4(ad) + H(ad)$: 4−9 μs $CH_4(ad) \rightarrow CH_3(ad) + H(ad)$: 0.09−0.22 ps $CH_3(ad) \rightarrow CH(ad) + H(ad)$: 37−91 ps $CH(ad) \rightarrow C(ad) + H(ad)$: 0.3−0.8 ns $CH(ad) \rightarrow C_2H_2$: 0.3−0.8 ns	2015 (ref 60)
Nucleation of a liquid argon droplet from a supersaturated argon vapor	CV: the total number of argon atoms in the liquid phase (e.g., coordination number >5). Classical MD with Lennard-Jones potential.	Computed first passage time of nucleation is between 10^{-6} and 10^{0} s. The nucleation rate is in order of magnitude agreement with large-scale simulations	2016 (ref 124)
Fuel Combustion Mechanism, pyrolysis and oxidation of n-dodecane	CVHD with ReaxFF force field, CV: Stretching degree of freedom of the C−C and C−H bonds.	(a) Pyrolysis time at 1000 K: 57 ns (b) combustion time at 700 K: 38 s	2016 (ref 63)
Monomer exchange in structural variants of a synthetic supramolecular polymer	All-atom and Coarse-Grained Model of polymers. 2D CV space: (i) the minimum distance and (ii) the coordination between the core of the activated monomer and the closest neighbors in the stack.	Spontaneous monomer incorporation (∼ns), slow monomer dissociation (∼10−100 ns) and medium-time scales for intermediate steps (∼10 nanosecond)	2017 (ref 127)
S_N2 reaction: $CH_3F + Cl^- \leftrightarrow CH_3Cl + F^-$	VRS Flooding with the difference between the C−F and C−Cl distances used as CV. Ab initio MD with PM6 semiempirical model.	Rate constants between 10^{-2} and 10^{3} s^{-1} for temperatures between 600 and 1200 K.	2017 (ref 64)
Hydrogen transfer reaction in compounds of chemical formula $C_nH_nO_n$	CV: various intramolecular distances such as C−H or C−O radical. AIMD with DFTB Hamiltonian.	Kinetics depends on the ring size of the transition state (TS). Activation barriers from Arrhenius plots of infrequent metadynamics are consistent with those obtained from climbing image nudged elastic band (CI-NEB) theory	2018 (ref 128)
Nanowall nucleation rate under hydrostatic tension of dicyclopentadiene (DCPD) polymer	CV: Number of cross-linkers with less than 5 coordination with neighbors. Force field: GAFF.	Nanowall nucleation rate about 10^{26} cm^{-3} s^{-1} corresponding to time scales of 10^{-6} s	2018 (ref 129)
Methane transport across antiagglomerant films	Classical MD simulation with TraPPE-UA force field. CV: Cartesian coordinates of the free methane molecule.	Characteristic time scale τ_{ss} is 0.01−1 μs	2018 (ref 130)
Ibuprofen Conformational Isomerism at the Crystal/Solution Interface	Classical MD with GAFF force field. CV: two internal torsional angles that represent global and local rearrangements of the ibuprofen molecular structure.	Conformational transition time scale in solution is 230 ns and 2−5 ns in the absorbed state, surface state, or crystal bulk state	2018 (ref 131)
Dehydrogenation in solid ammonia borane	AIMD at DFT level of theory with PBE functional. CV: Coordination number between the two H atoms to monitor H_2 formation.	Hydrogen evolution time scale of ∼0.8 ns	2019 (ref 80) plumID:19.082
Toluene Oxidation and Pyrolysis in the presence of external electric field	CV: distance of C−C bond (pyrolysis) or C−H bond (oxidation). MD simulation with ReaxFF forcefield.	Reaction time scales obtained from infrequent metadynamics follow Arrhenius's behavior.	2019 (ref 132)
Urea Decomposition in aqueous media.	Born−Oppenheimer molecular dynamics (BOMD) at DFT level with PBE functional. Bias applied along a Path CV s defined as a function of permutation invariant descriptors composed of coordination numbers between C−N and N−H bonds.	The decomposition rates at 390 and 490 K were found to be 4.46 × 10^{-5} and 3.02 × 10^{-4} s^{-1}, respectively	2019 (ref 133)
liquid droplet nucleation in Argon	Ll potential. SGOOP CV trained on 3 descriptors: (1) the total number of liquid argon atoms in the system, (2) the second moment of coordination number, (3) the third moment of coordination number.	Nucleation rate between 10^{25} cm^{-3} s^{-1} and 10^{27} cm^{-3} s^{-1} (2) the second moment of coordination number, (3) the third moment of coordination number.	2019 (ref 134)
Monomer transition in supramolecular tubule	Coarse-grained (CG) model of the tubule solvated in MARTINI water. CV: central C-N−N-C dihedral angle in the azobenzene tail units.	Trans-to-cis tail transition in perfect tubule: approx 100 s CG time	2019 (ref 135)
Supramolecular Catalysis of m-Xylene Isomerization by Cucurbituril	AIMD. CV: Coordination number between carbon atoms	Rate constants consistent with Arrhenius Law for a range of temperature	2020 (ref 136)
Markovnikov (2-bromopropane) and anti-Markovnikov (1-bromopropane) hydrobromination of propene	GAMBES method: AIMD with PM6 Hamiltonian. Descriptor set with 5 interatomic distances between HBr	First passage time to the Markovnikov product: 6.1 × 10^2 hours	2020 (ref 30) plumID:20.014

… and more …

CV based approach: Infrequent metadynamics

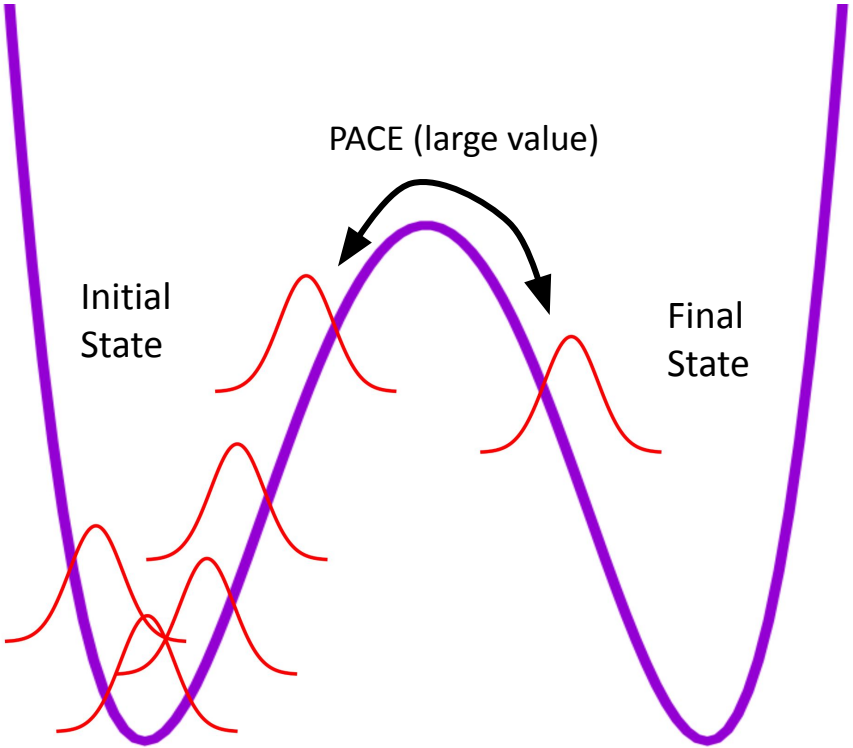

- Metadynamics with higher PACE (low frequency of Gaussian bias deposition)
- “Hope” that no bias will be deposited on TS which is short-lived

Tiwary and Parrinello PRL 2013, Salvalaglio et al. JCTC 2014

And a large body of literature in biology, material and chemical systems

- **Less control on bias deposition**
- **Very slow progress due to less biasing**

OPES flooding

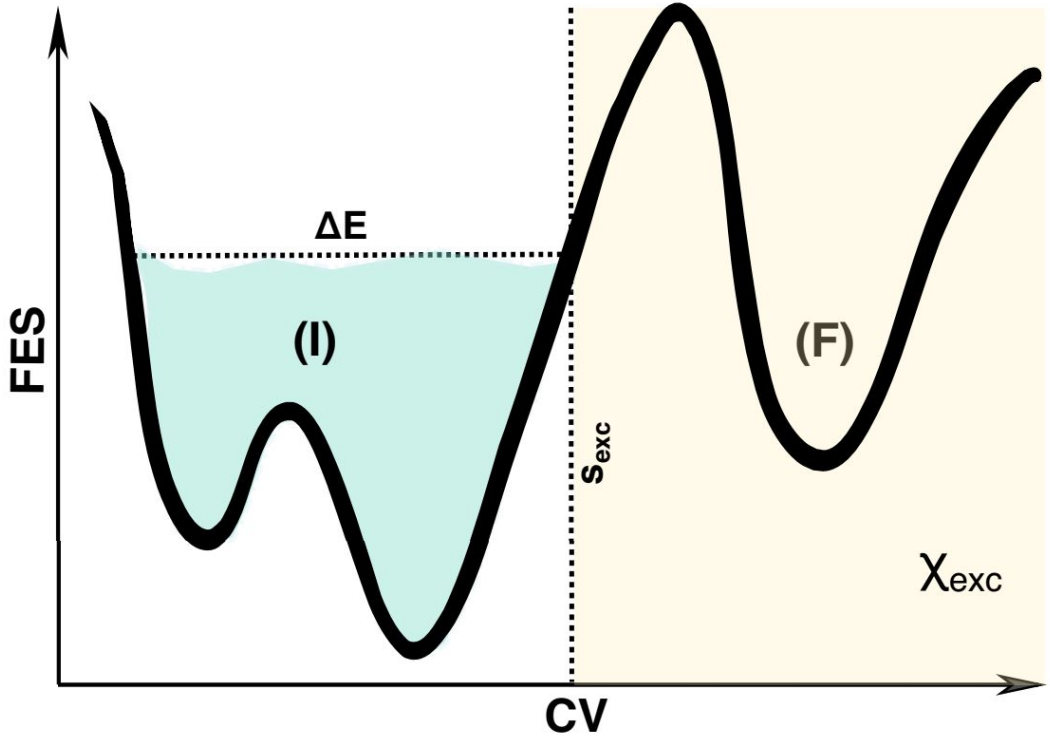

- Using OPES to bias and fill the initial state basin (I)
- Explicit BARRIER (**ΔE**) parameter limits bias deposition
- Explicit excluded region (χ_{exc}) to avoid biasing TS
- Trajectory stopped after successful transition (I to F)
- **More control over "where" and "how much" to bias**

OPES: Invernizzi, M., & Parrinello, M. JPC Lett (2020)
OPES Flooding: Ray, D., Ansari, N., Rizzi, V., Invernizzi, M., & Parrinello, M. JCTC (2022)

Practical Rare Events involve barrier crossing and diffusion

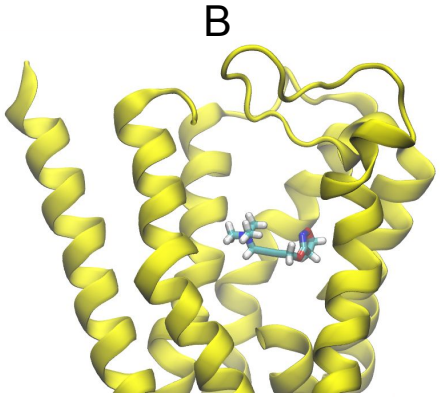

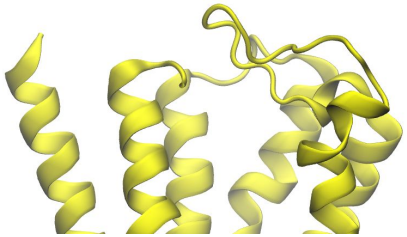

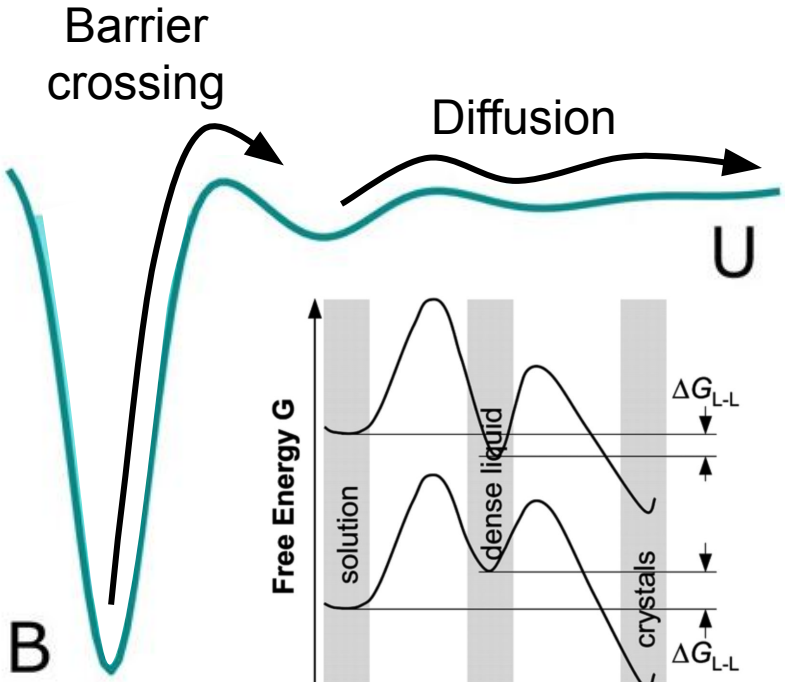

Peter G. Vekilov
Crystal Growth & Design 2004

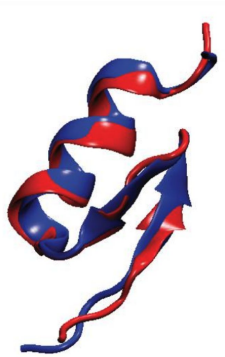

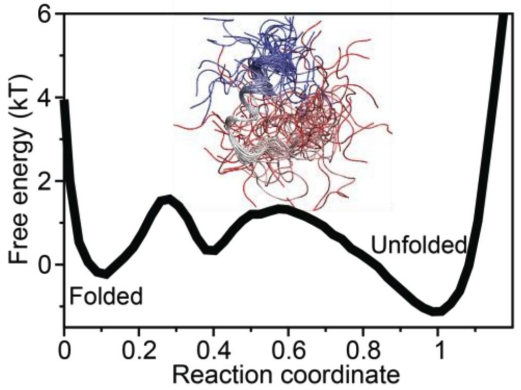

Lindorff Larsen et al. Science 2011

Practical Rare Events involve barrier crossing and diffusion

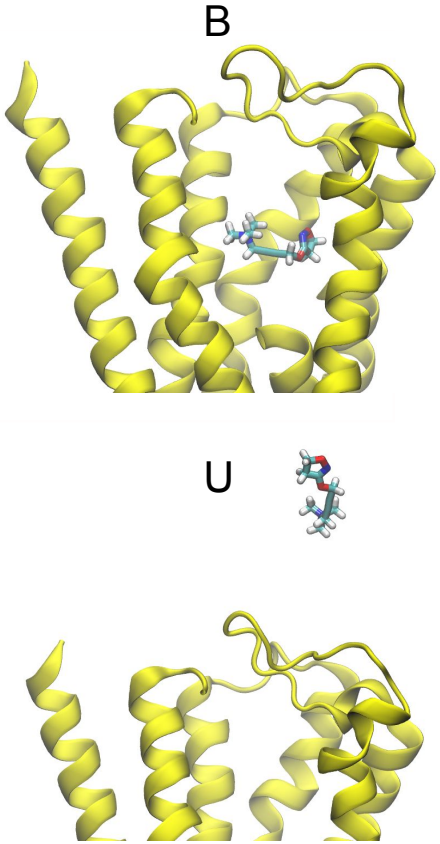

Often we know only the structure of the initial state

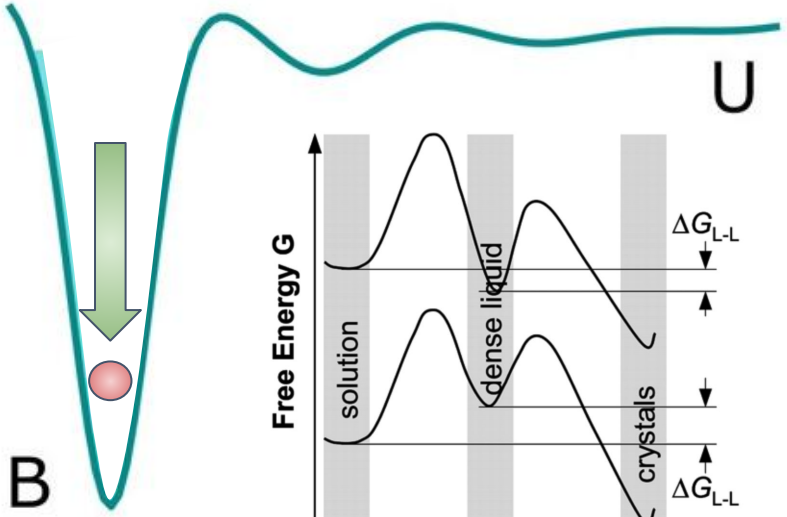

Peter G. Vekilov
Crystal Growth & Design 2004

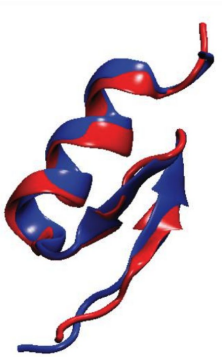

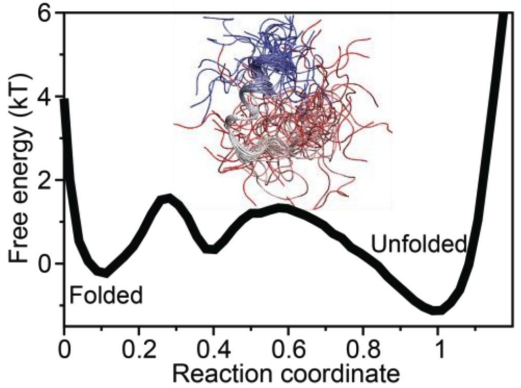

Lindorff Larsen et al. Science 2011

Limitation of OPES flooding (biased Enhanced Sampling)

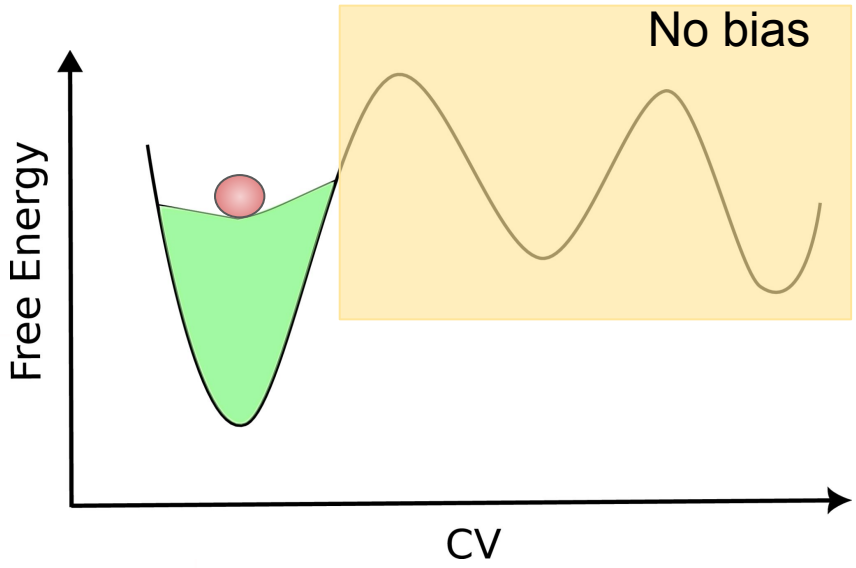

OPES-Flooding setup

Limitation of OPES flooding (biased Enhanced Sampling)

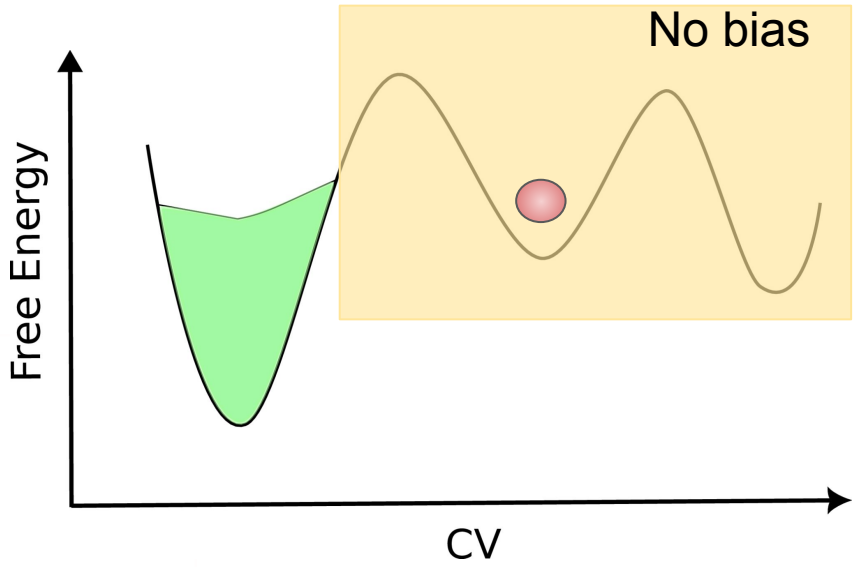

No mechanism of accelerating the dynamics
beyond the initial state minimum

Limitation of OPES flooding (biased Enhanced Sampling)

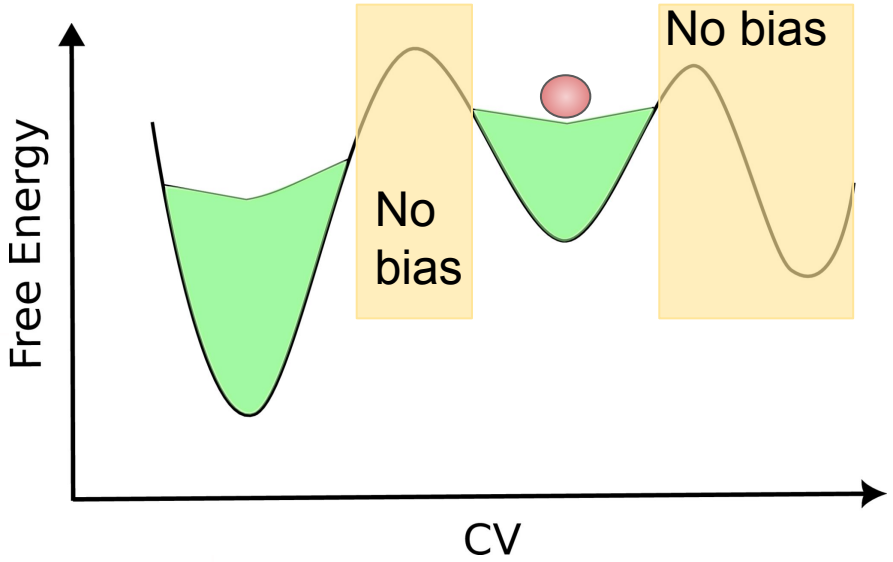

But then we need to know the precise free energy surface

1. Computationally expensive. 2. We only want the kinetics

Limitation of OPES flooding (biased Enhanced Sampling)

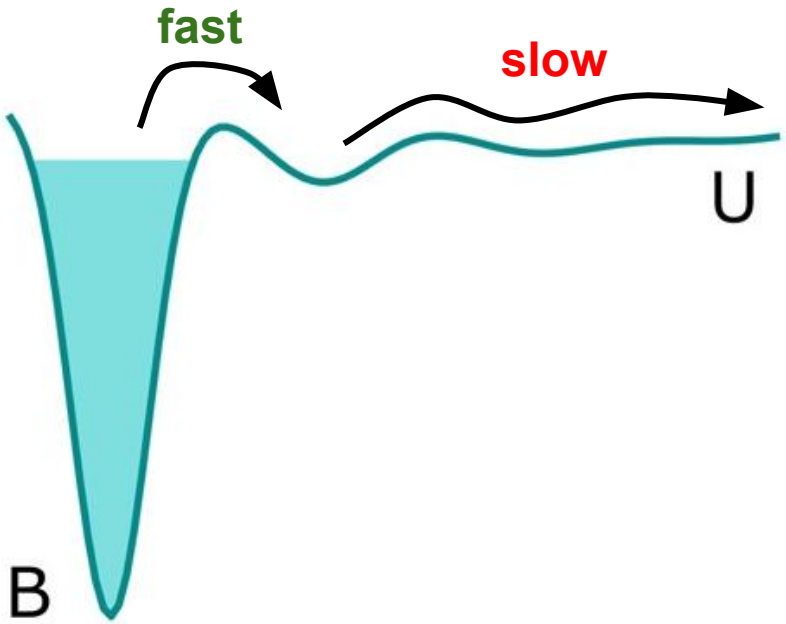

Biased Enhanced Sampling (e.g. OPES-Flooding)

✅ Crossing Steep Barrier

❌ Exploring Diffusion in Rugged Free Energy Landscape

✅ ❌ Kinetics (sometime but difficult)

Weighted Ensemble Method

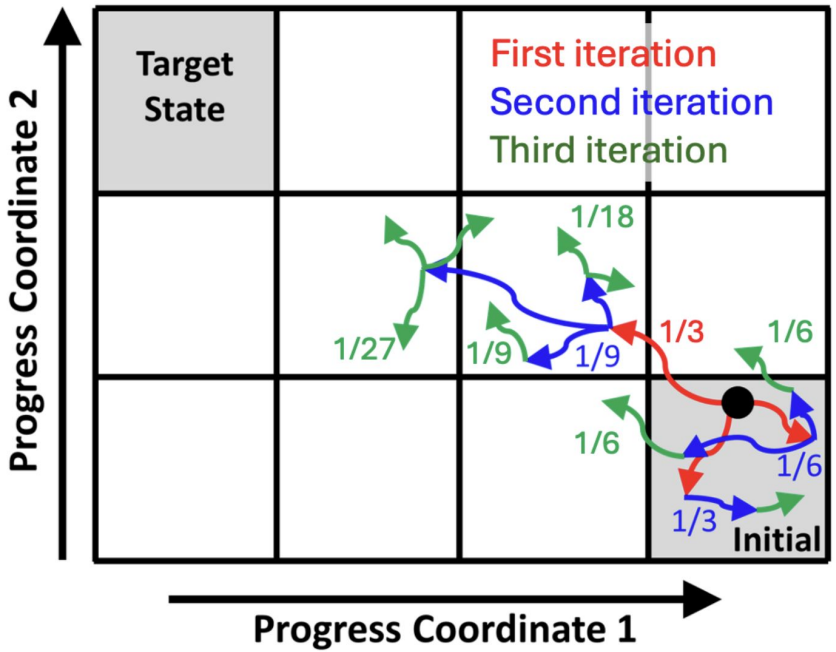

Trajectories are split or merged upon crossing into a new bin with weights adjusted

Huber & Kim, JCP (1996), Zhang et al. JCP (2010), Figure: Chong and Zuckerman, ChemRxiv (2025)

Weighted Ensemble is less efficient in steep barrier crossing

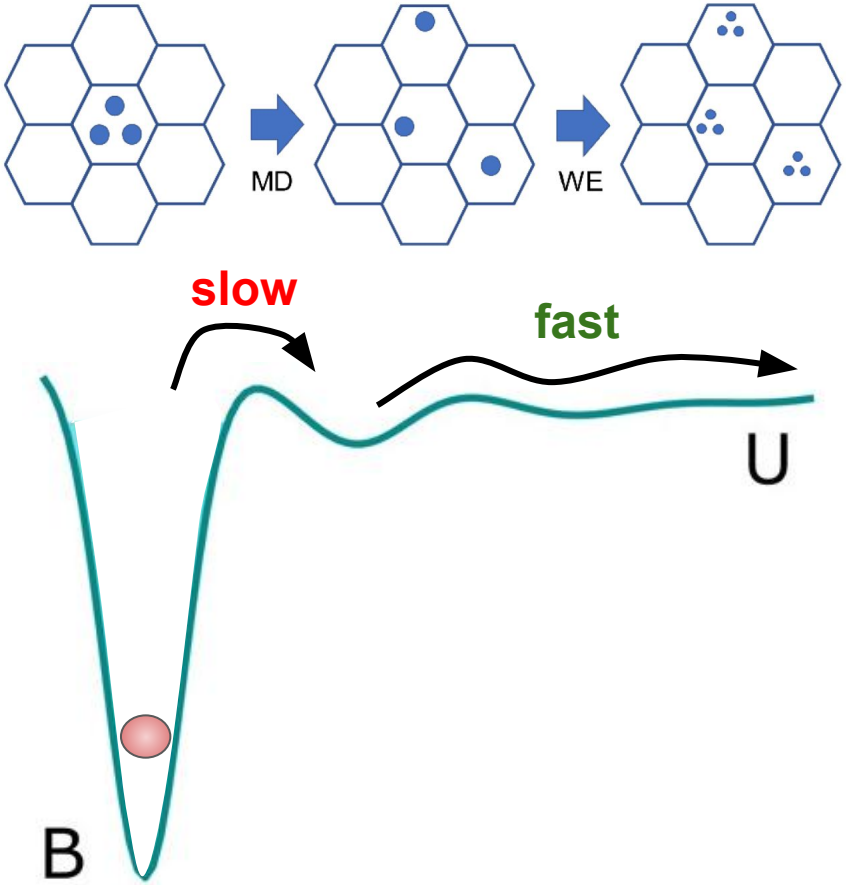

Unbiased Path Sampling (e.g. Weighted Ensemble)

❌ Crossing Steep Barrier

✅ Exploring Rugged Free Energy Landscape

✅ ❌ Kinetics

Solution: Integrated Sampling

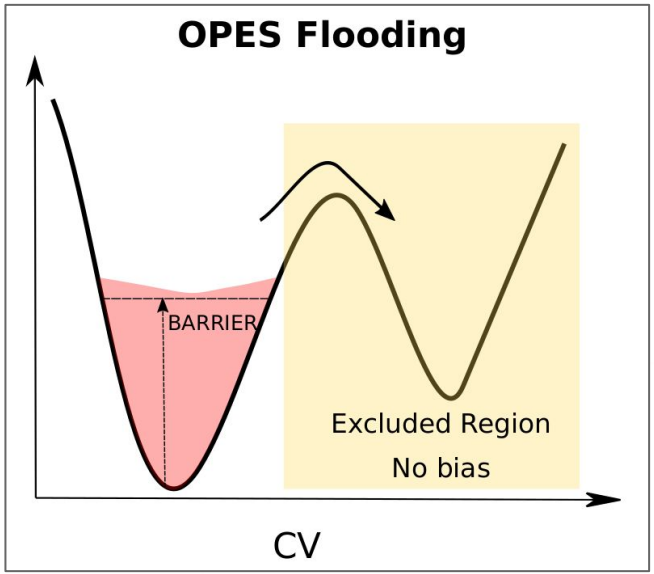

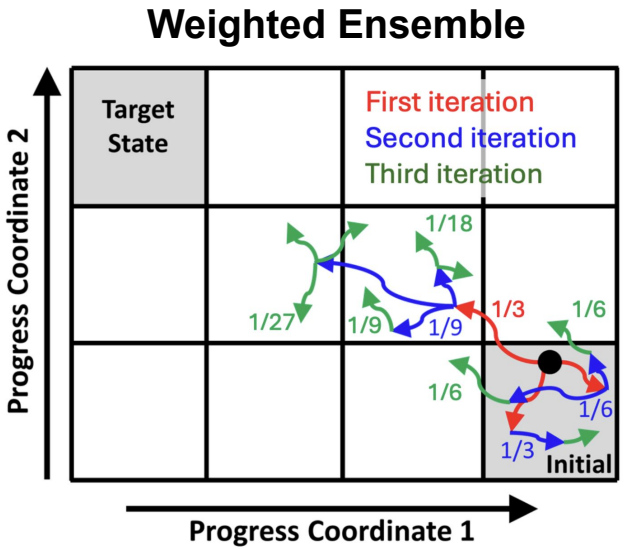

Solution: Integrated Sampling

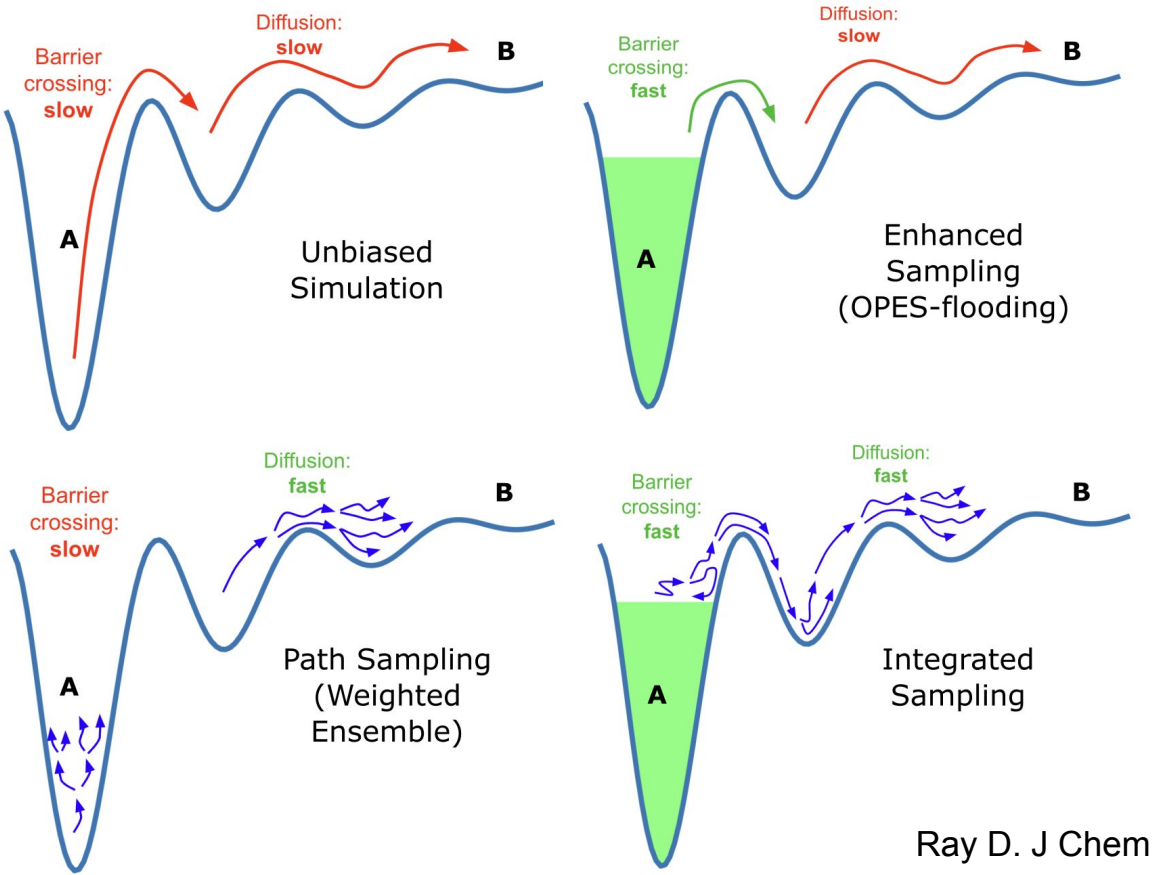

Ray D. J Chem Phys (2024)

Tracing and Rescaling successful transitions

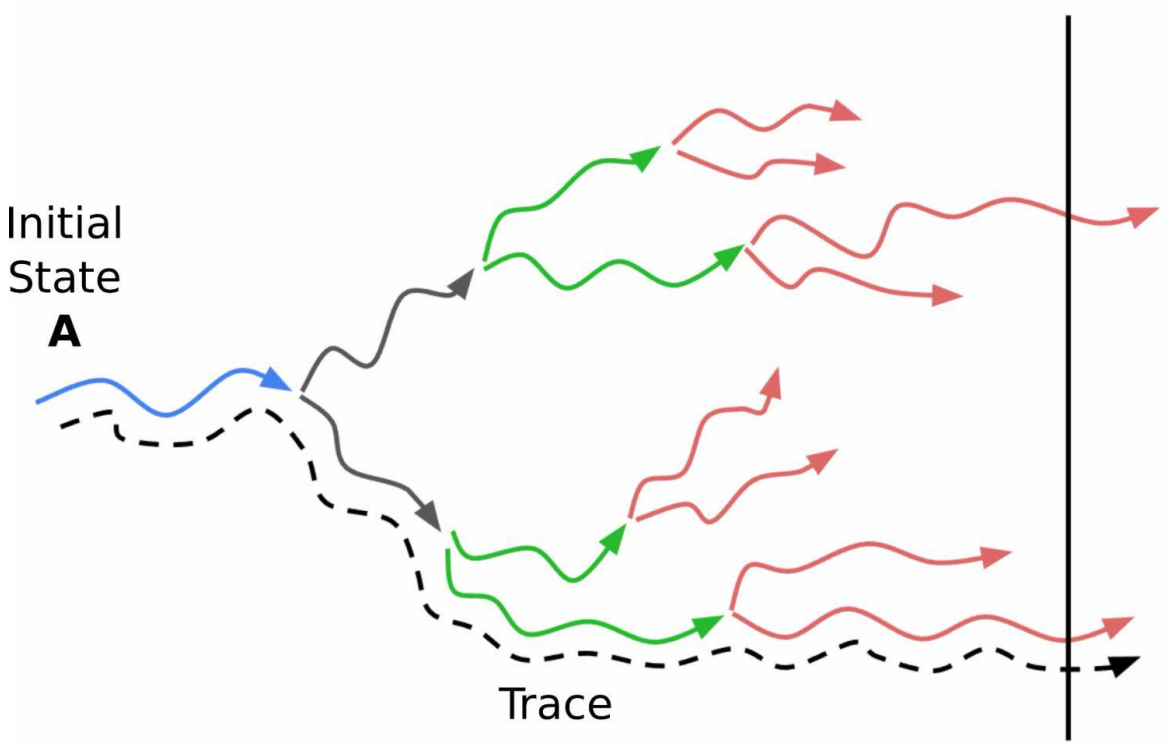

$$\langle \tau \rangle = \frac{\sum_k^M w_k \tau_k}{\sum_k^M w_k}$$

$$\tau = \sum_i^{N_{tot}} \Delta t \exp(\beta V(\mathbf{s}_i))$$

Ray D. J Chem Phys (2024)

Results: Gas Phase Alanine Dipeptide

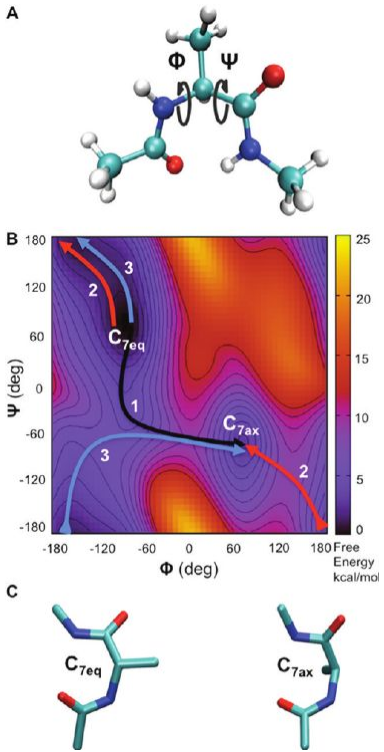

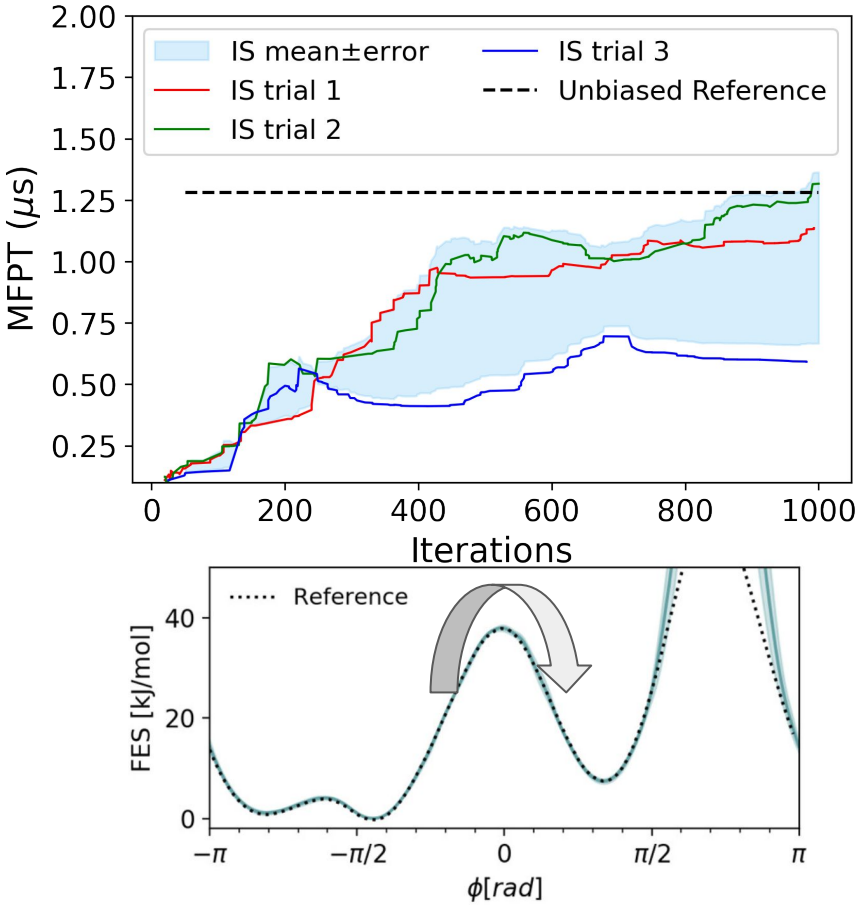

Method	Simulation time
OPES-flooding (30 transitions)	10.6 ns
Integrated Sampling (500 iterations)	**21 ns**
Infrequent Metadynamics (20 transitions)	54 ns
WE (3000 iter) 1 transition	> 100 ns

Ray D. J Chem Phys (2024)

Results: Chignolin Unfolding

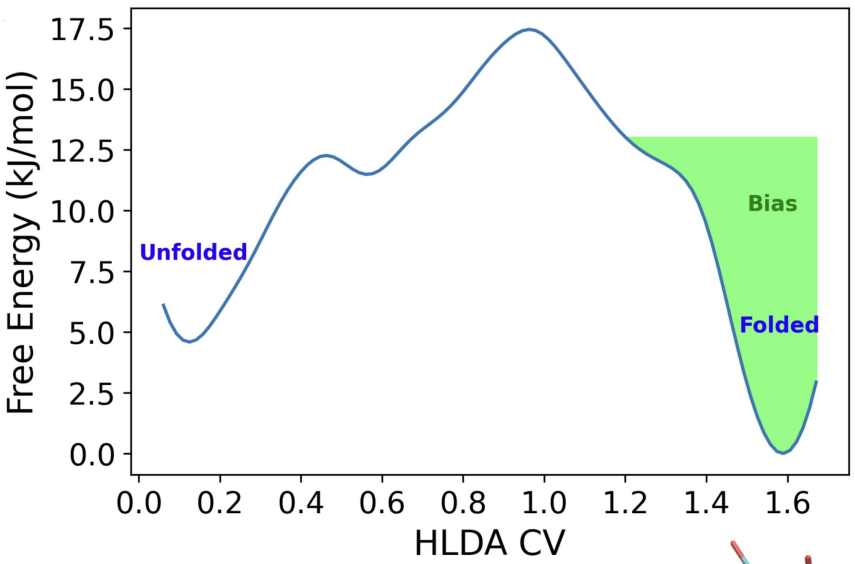

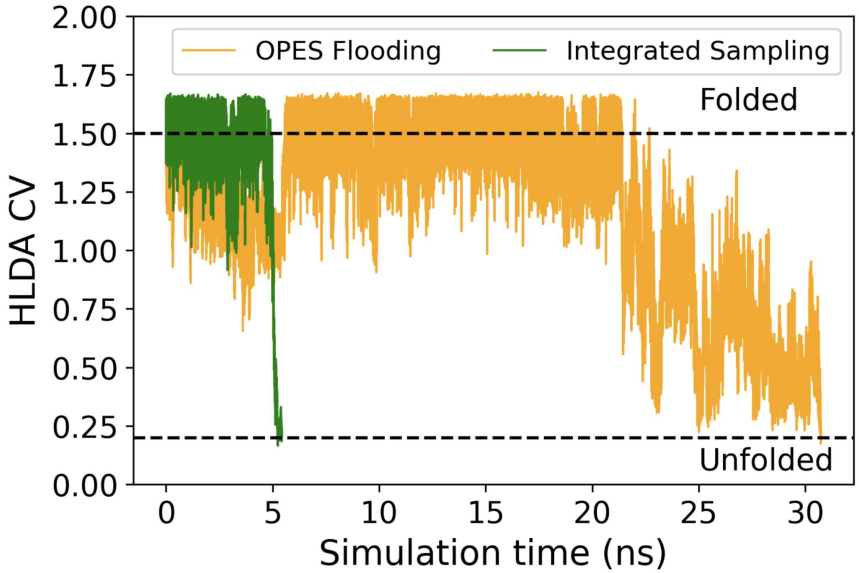

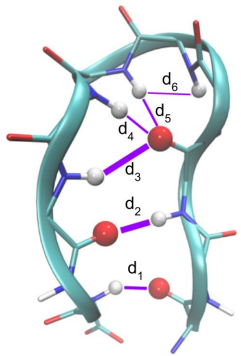

Mendels et al. JCP 2018

Ray D. J Chem Phys (2024)

Results: Chignolin Unfolding

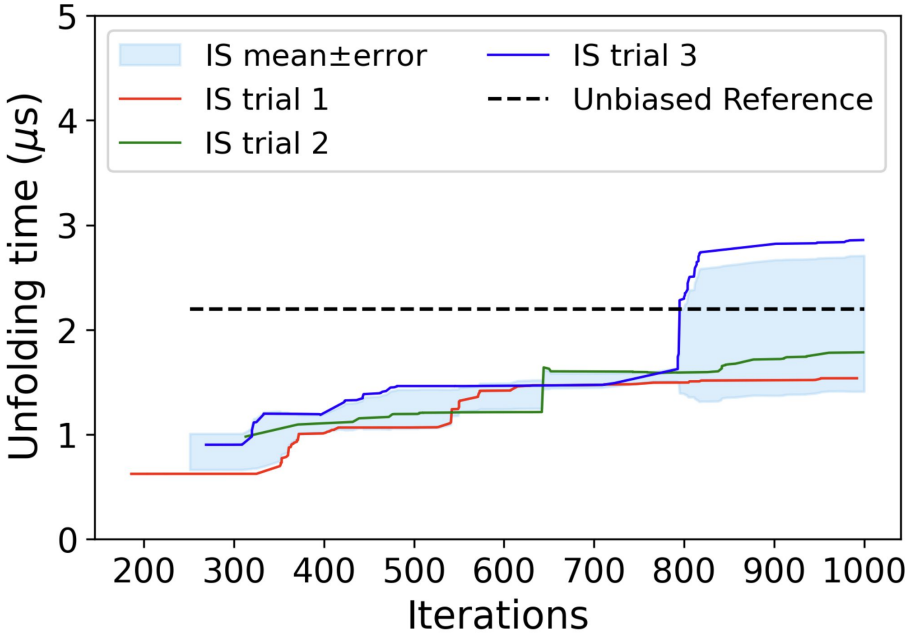

Method	Unfolding time (μs)	Simulation time
OPES-flooding (15 transitions)	6.3	825 ns
Integrated Sampling (1000 iterations)	**1.8**	**460 ns**
Infrequent Metadynamics (20 transitions)	33.7	237 ns
Reference (DE Shaw)	2.2	> 100 μs

Ray D. J Chem Phys (2024)

Results: Chignolin Unfolding

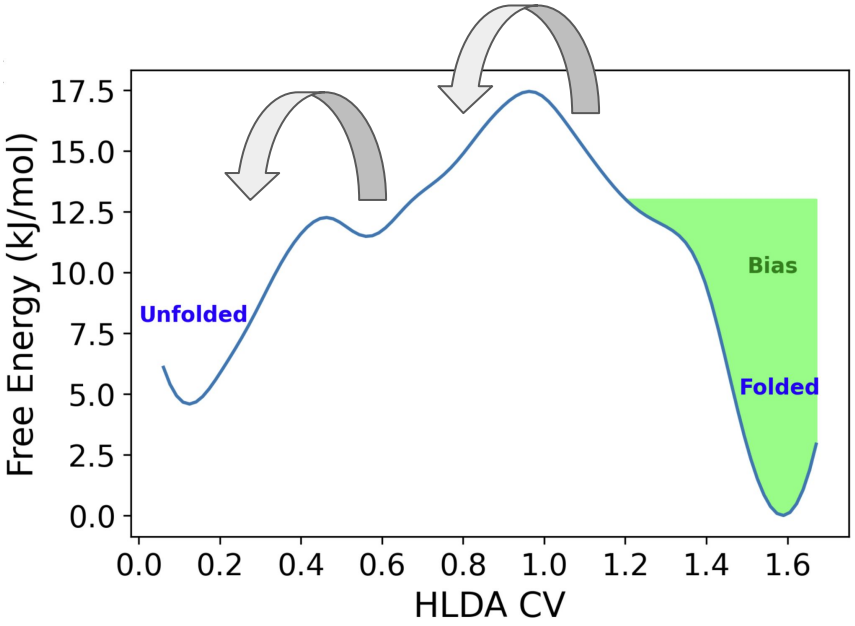

Method	Unfolding time (μs)	Simulation time
OPES-flooding (15 transitions)	6.3	825 ns
Integrated Sampling (1000 iterations)	**1.8**	**460 ns**
Infrequent Metadynamics (20 transitions)	33.7	237 ns
Reference (DE Shaw)	2.2	> 100 μs

Ray D. J Chem Phys (2024)

Results: Ligand Receptor (Host-Guest) Unbinding

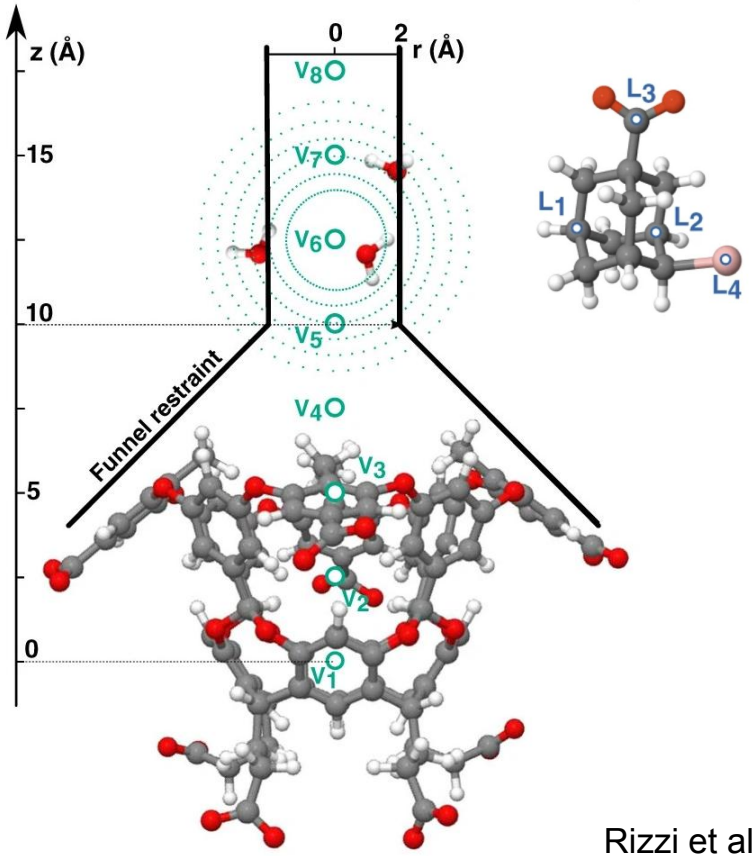

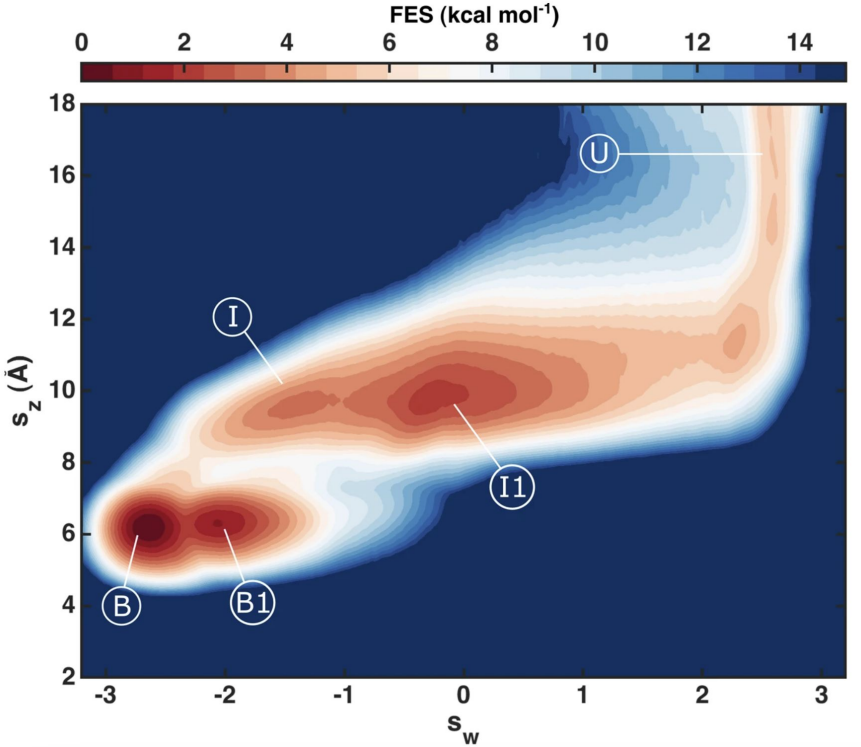

Deep LDA Water CV

Rizzi et al. *Nat. Comm.* 2021

Results: Ligand Receptor (Host-Guest) Unbinding

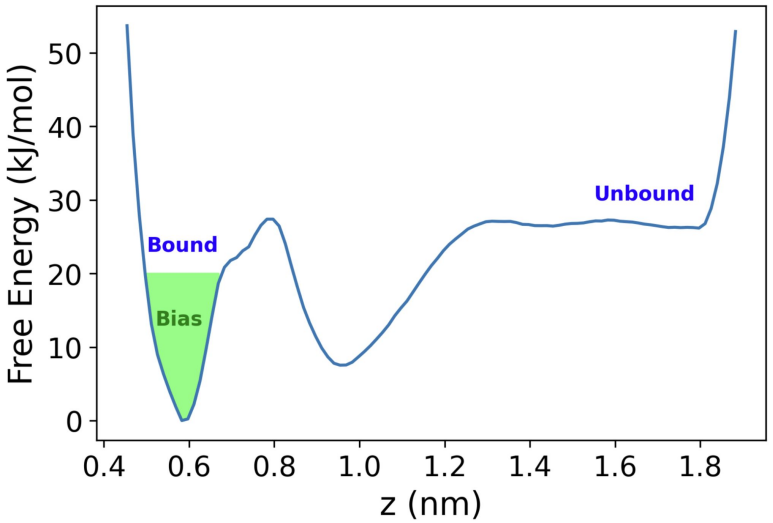

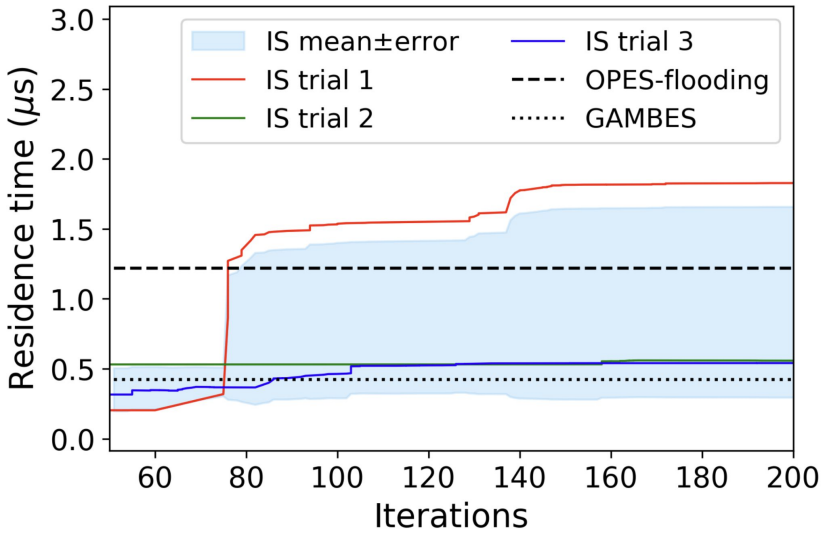

Method	Residence time (μs)	Simulation time
OPES-flooding (30 transitions)	0.8-1.8	500 ns
Integrated Sampling (200 iterations)	**1.0 +/- 0.7**	**~90 ns**

Ray D.
J Chem Phys
(2024)

Results: Ligand Receptor (Host-Guest) Unbinding

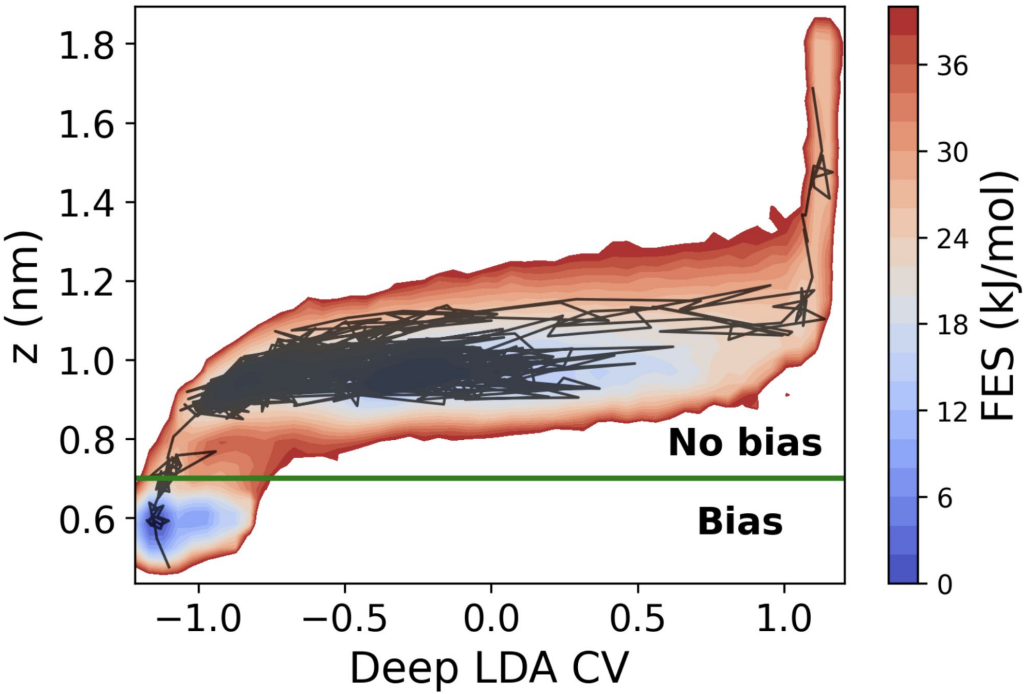

Highest weight path follows the minimum free energy pathway along the z vs water CV space.

Water role is captured without explicitly defining it in the progress coordinate. (**Suboptimal CV**)

Ray D. J Chem Phys (2024)

Realistic Application: HSP90 Protein Conformational Transition

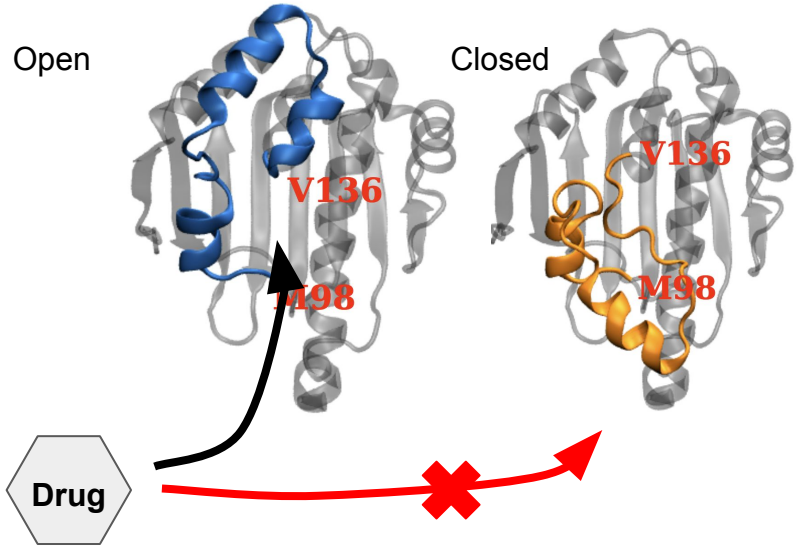

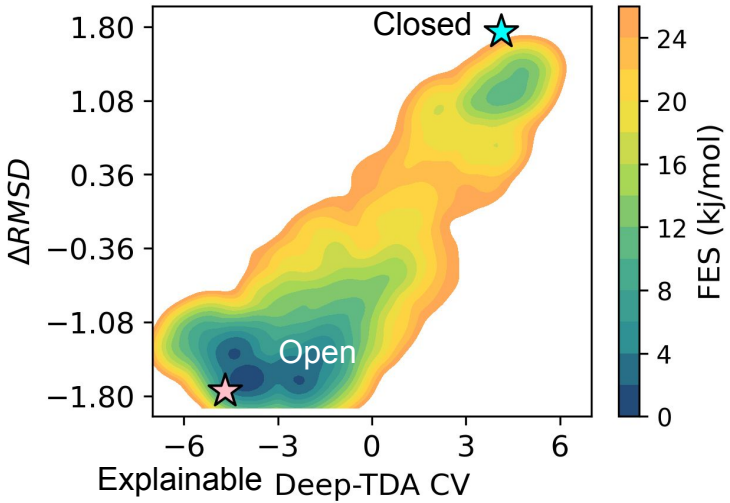

Dr. Sompriya Chatterjee

Henot F. et al.; Nat. Comm 2022

Chatterjee S. and Ray D. JCTC 2025

Chatterjee S. and Ray D. under preparation

Method	Open to closed rate constant (s^{-1})
Experimental	81 ± 12
Integrated Sampling (~1.5 μs)	**14 ± 4**
OPES-Flooding (>2 μs)	No transition

Conclusions

1. Integrated Sampling (i.e. WE + OPES-flooding) can **efficiently calculate kinetics** in systems involving both barrier crossing and diffusion.
2. **Choice of CV not very critical.**
3. We can deposit bias conservatively without loss of efficiency
4. Drive transitions through minimum energy pathways

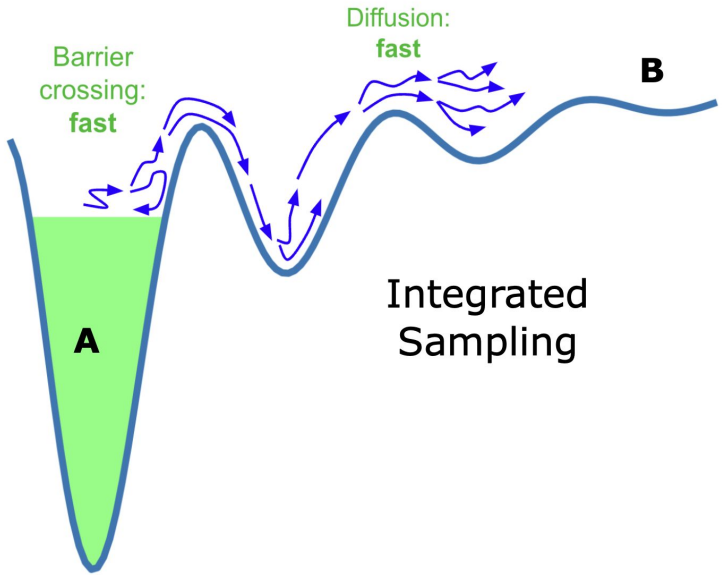

Ray D. J Chem Phys (2024)

Open Source Implementation

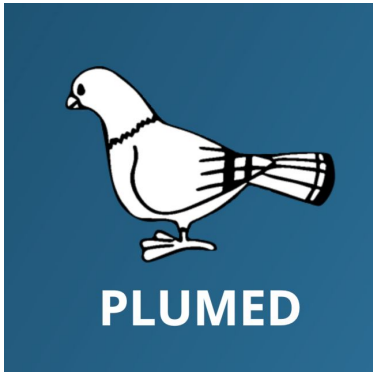

The PLUMED consortium. Promoting transparency and reproducibility in enhanced molecular simulations, Nat. Methods 16, 670 (2019)

Bogetti, Anthony T., Jeremy M. G. Leung, John D. Russo, She Zhang, Jeff P. Thompson, Ali S. Saglam, **Dhiman Ray**, et al. 2023. “A Suite of Tutorials for the WESTPA 2.0 Rare-Events Sampling Software [Article v2.0]”. Living Journal of Computational Molecular Science 5 (1)

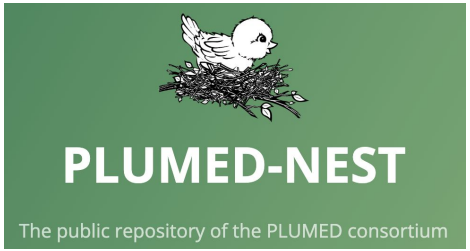

plumID	Name	Category	Keywords	Contributor
24.022	Integrating Path Sampling with Enhanced Sampling for Rare-event Kinetics	methods	OPES Flooding, Weighted Ensemble, Metadynamics, Kinetics, Infrequent Metadynamics, Integrated Sampling	Dhiman Ray

Future Direction

1. Calculating Free Energy landscape using combined WE and OPES.

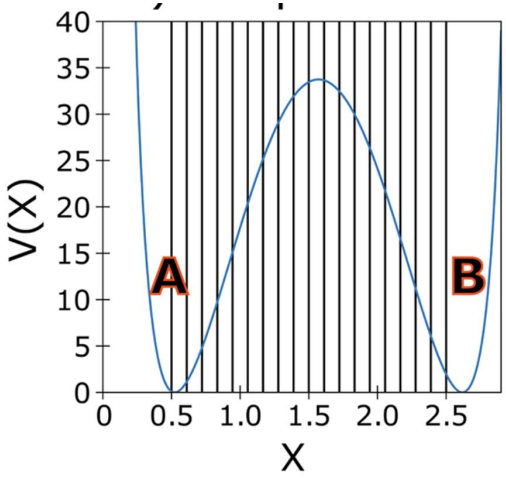

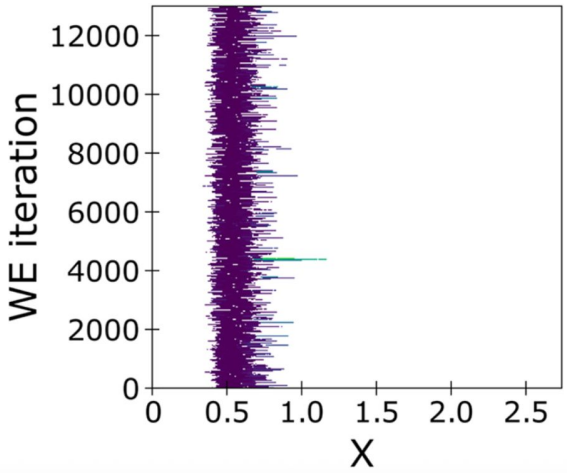

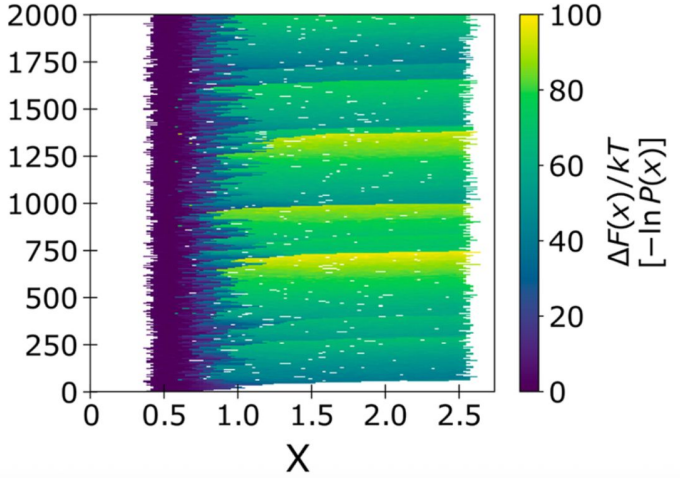

Future Direction

1. Calculating Free Energy landscape using combined WE and OPES.
2. Solving the trajectory correlation problem

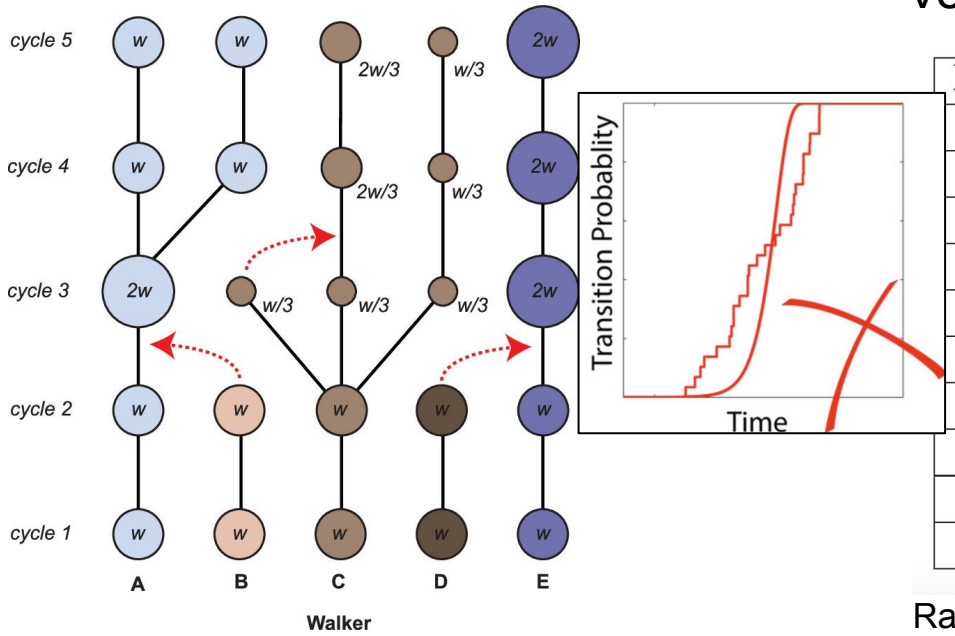

Very high number of transitions

Iteration	Trial 1	Trial 2	Trial 3
100	0	115	64
200	30	347	235
300	120	612	398
400	313	826	554
500	517	1058	711
600	726	1232	884
700	958	1404	1013
800	1162	1515	1109
900	1359	1630	1265
1000	1479	1770	1382

Ray, JCP (2024), Bose et al. JCTC (2025)

Acknowledgements

UNIVERSITY OF OREGON

PostDoc

Dr. Sompriya Chatterjee

Graduate Students

Revanth Elangovan

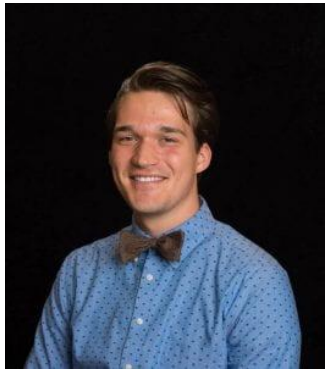

Jack Hanni